Global and regional climate feedbacks in response to uniform warming and cooling

Mark A. Ringer, Alejandro Bodas-Salcedo, and Mark J. Webb

Met Office Hadley Centre, Exeter, U.K.

Corresponding author: Mark Ringer (mark.ringer@metoffice.gov.uk)

Key Points:

- The global climate feedback is less stabilising under warming compared to cooling.
- This behaviour is primarily driven by the responses of clouds and water vapour in the tropics.
- Simplified climate model experiments are a valuable tool to help us understand climate feedbacks in colder and warmer climates.

Abstract

We compare the radiative feedbacks resulting from a uniform warming and cooling of sea surface temperatures by 4 K in an ensemble of global climate models. The global-mean net feedback is less stabilising in response to warming in all nine models. This is primarily due to a stronger tropical water vapour feedback, with a smaller contribution from the shortwave cloud feedback. The zonal-mean feedbacks are similarly robust across the ensemble. In the extra-tropics, more positive shortwave cloud feedback under warming is associated with further poleward migration of the mean Southern Hemisphere jet latitude in some models. However, additional experiments with an aquaplanet version of the HadGEM3 model suggest that the asymmetry of the jet shift is not driving that in the cloud feedbacks at these latitudes. In the tropics, stronger water vapour feedback under warming is offset by a weaker shortwave cloud feedback. The result is that the ensemble spread in the differences between the global feedbacks under warming and cooling is mainly determined by their differences in the tropics. The spatial distribution of the feedbacks largely reflects the zonal mean behaviour, although there is considerable intermodel variation in the regional cloud feedbacks, particularly in the tropical shortwave cloud feedback. Comparison with CO_2- and solar-forced coupled experiments suggests that the global-mean longwave cloud feedback is nearly invariant to warming and cooling, regardless of the nature of the forcing. The shortwave cloud feedback is generally more positive under warming in the coupled models, consistent with the uniform SST perturbation experiments.

Plain Language Summary

A longstanding question in climate science is whether the study of cooler past climates can help us to understand future climate change in response to increasing CO_2 and other greenhouse gases. Answering this question is difficult because when the Earth was much colder the climate itself was quite different from today's. This means that we cannot be sure that feedbacks in the climate system operated as they do now, or as they might do in the future. To simplify the problem we have examined climate model experiments in which the surface temperature of the oceans is alternately warmed and cooled by a fixed amount relative to the present day. This provides us with a baseline for understanding the differences between more realistic scenarios of past and future climates. We highlight the role of clouds and atmospheric water vapour in determing these differences and the relative importance of the tropics compared to higher latitudes.

1 Introduction

Do past, cooler climates provide us with useful insights into future global warming? This depends to a large degree on whether climate feedbacks are "symmetric". That is, if warming and cooling of the same magnitude lead to equal and opposite responses. We also need to account for known asymmetries in the forcing, such as the location and extent of the major ice sheets or changes in the Earth's orbit around the Sun.

Recognising these complexities, the Cloud Feedback Model Intercomparison Project (CFMIP; Webb et al., 2017) includes a simple uniform cooling experiment in which SSTs are everywhere reduced by 4 K from their present-day values. This complements the standard warming experiment in which SSTs are increased by 4 K. The aims are to isolate the basic responses to warming and cooling, identify any fundamental differences between the resulting feedbacks, and provide a baseline for comparisons of more realistic past and future climates.

We can identify two kinds of asymmetry: (i) feedbacks could have the same sign but different magnitudes under warming and cooling, or (ii) feedbacks could have the opposite sign. In practice we find that (ii), which is clearly a more complex physical situation, rarely occurs at the global scale in the models we examine here, although we note one or two examples. Local asymmetry in the feedbacks is, however, more common, particularly in relation to cloud feedbacks.

The first global climate model (GCM) study to examine such idealized scenarios was Schneider et al. (1978), who described uniform 2 K SST warming and cooling experiments with the NCAR model for perpetual January conditions. They found symmetric cloud feedbacks in response to cooling and concluded that this added confidence to the results they obtained under warming.

Cess et al. (1990) also performed uniform SST +/-2 K experiments, this time for perpetual July conditions, to examine cloud feedbacks in an ensemble of climate models. Their focus, however, was to use the 4 K SST difference to increase the signal-to-noise ratio for the feedback calculation, i.e., there was an implicit assumption of symmetry. The experiments continued to be used in this way when they were adopted by CFMIP (Ringer et al., 2006).

More recently, both Ringer et al. (2014) and Qin et al. (2022) demonstrated the value of uniform SST +4 K warming experiments for interpreting feedbacks in fully coupled models under the *abrupt-4xCO2* scenario, providing motivation that uniform cooling experiments might be similarly informative.

Yoshimori et al. (2009) compared Last Glacial Maximum (LGM) and 2xCO2 simulations using the MIROC 3.2 model coupled to a 50 m mixed layer ("slab") ocean and described a framework for analysing the responses to warmer and cooler climates. They included an experiment in which only the greenhouse gas concentrations were set to LGM levels i.e., the ice sheets and other boundary conditions were left at their control values: this allowed them to examine the model's feedbacks in response to warming and cooling more generally. They found that the difference in the climate sensitivity between warming and cooling was due to a weakening of the positive shortwave cloud feedback under cooling, and in their full LGM experiment the sign of the global shortwave cloud feedback actually reversed.

The continuing relevance of understanding the climate response to global cooling is emphasised by Sherwood et al. (2020), who show that the LGM provides the strongest constraint

on the upper end of their Effective Climate Sensitivity (ECS) distribution. They make assumptions about the state dependence of feedbacks, that they are not the same for warming and cooling, which are based on comparisons of proxy evidence for warm and cold climates.

Here we examine a nine-member ensemble of uniform 4 K SST warming and cooling experiments submitted to CFMIP3/CMIP6 to address the three aims listed above. Our focus is on the robust differences between feedbacks under warming and cooling across the ensemble, although we do consider some aspects of model spread and diversity. We also compare global feedbacks and climate sensitivity estimates between these experiments and both CO_2- and solar-forced coupled-model warming and cooling scenarios. These are themselves idealised experiments which aim to provide insights into past climates, e.g., the CO_2-forced experiments are analogous to the Yoshimori et al. greenhouse gas only simulation. Recent studies using these idealised warming and cooling experiments have suggested that asymmetries in the global surface temperature response are driven primarily by the forcing (Mitevski et al., 2022), the feedbacks (Bloch-Johnson et al., 2021), or a combination of both (Chalmers et al., 2022).

The value of the uniform warming and cooling simulations is not necessarily to establish whether feedbacks are different under warming and cooling but rather to see if these differences can be reproduced in such an idealised framework: they are a component of the wider experimental hierarchy designed to increase our understanding of global climate feedbacks.

2 Data and Methods

The control experiment for this analysis is the standard *amip* simulation for the period January 1979 to December 2014. The perturbation experiments are uniform warming (*amip-p4K*) and cooling (*amip-m4K*), respectively, of the SSTs by 4 K over the same period, with the sea-ice distribution remaining unchanged. A full description of the CFMIP experimental protocols is given in Webb et al. (2017).

Radiative feedbacks in the warming and cooling experiments are defined as the differences in the top-of-atmosphere fluxes from the *amip* simulation divided by the global-mean change in the surface air temperature, ΔT. Note that the magnitude of ΔT is greater than 4 K because the land is free to respond to the warming and cooling. We also consider analogous aquaplanet versions of these experiments (*aqua*, *aqua-p4K*, *aqua-m4K*) using the HadGEM3-GC3.1-LL model (Section 5), in which the feedbacks are estimated in the same way.

In addition, we derive feedbacks and radiative forcing from CO_2- and solar-forced coupled model experiments: *abrupt-2xCO2*/*abrupt-0.5xCO2* and *solar-p4p*/*solar-m4p*. These are also part of CFMIP and are described in Webb et al. (2017). In this case the global-mean feedbacks are estimated using 150 years of annual mean differences from the corresponding *piControl* experiments – the "Gregory plot" (Gregory et al., 2004).

Differences between the ensemble-mean *amip-p4K* and *amip-m4K* responses are tested using a two-sided *t*-test, the null hypothesis being that the expected difference is zero. Given the small sample size of nine models, we take a cautious approach and only consider statistical significance at the 1% level ($p < 0.01$) to be indicative of robust differences between the responses to warming and cooling.

We first consider the global-mean responses and feedbacks (Section 3), then examine the regional responses in more detail (Section 4). In Section 5 we discuss the poleward shift of the mid-latitude jet in the Southern Hemisphere and its relationship to cloud feedbacks. Finally, in

Section 6, we compare global-mean feedbacks and estimates of effective climate sensitivity from the uniform SST experiments with the CO_2- and solar-forced coupled model warming and cooling scenarios. Our conclusions are summarized in Section 7.

Table 1: Surface air temperature changes for the *amip-p4K* and *amip-m4K* experiments. Values are 36-year means for the period January 1979 – December 2014.

	Globe, K		Land, K		Land / Ocean	
	p4K	**m4K**	**p4K**	**m4K**	**p4K**	**m4K**
BCC-CSM2-MR	4.53	-4.35	5.70	-5.25	1.41	1.32
CESM2	4.32	-4.15	5.24	-4.68	1.33	1.19
CNRM-CM6-1	4.52	-4.39	5.67	-5.33	1.40	1.33
CanESM5	4.59	-4.33	5.65	-5.11	1.36	1.27
GFDL-CM4	4.57	-4.44	5.58	-5.17	1.34	1.25
HadGEM3-GC31-LL	4.43	-4.25	5.50	-4.94	1.38	1.25
IPSL-CM6A-LR	4.32	-4.22	5.10	-4.83	1.28	1.22
MRI-ESM2-0	4.49	-4.41	5.32	-4.99	1.28	1.20
TaiESM1	4.58	-4.47	5.60	-5.18	1.34	1.24
Mean	**4.48**	**-4.34**	**5.48**	**-5.05**	**1.35**	**1.25**
Standard deviation	**0.10**	**0.11**	**0.21**	**0.21**	**0.05**	**0.05**

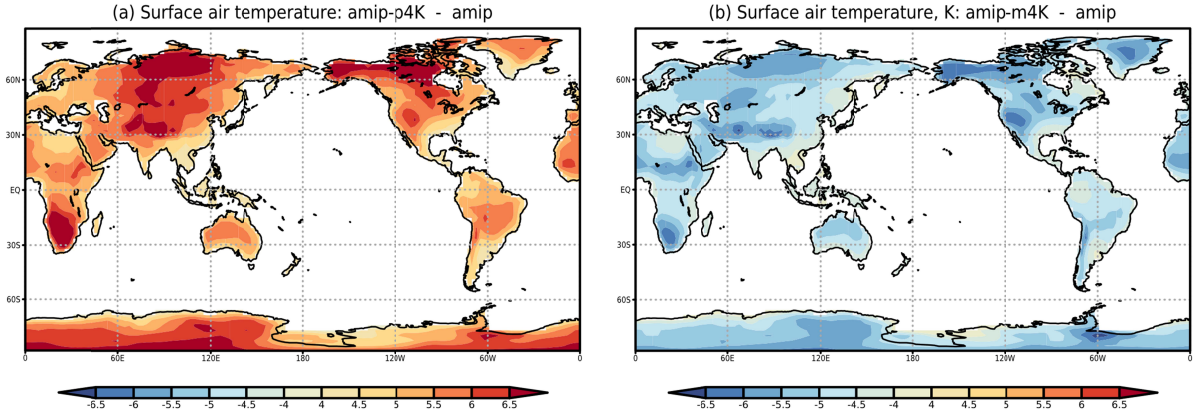

Figure 1: Ensemble mean surface temperature change in the (a) *amip-p4K* and (b) *amip-m4K* experiments (K). Values are annual means relative to *amip* for the period January 1979 – December 2014.

151 **3 Global responses**

152 3.1 Surface warming

153 Differences between the magnitude of the global-mean surface warming and cooling are
154 relatively small in the nine models we examine here (Table 1), and are, by design, driven by the
155 differences over land (Figure 1). Nonetheless, both the global-mean difference of 0.15 K and the
156 0.4 K difference in the magnitude of the land surface temperature change are statistically
157 significant at the 1% level. The ensemble-mean ratio of the land to ocean temperature changes
158 (the "land/sea contrast") is 1.35 in *amip-p4K* and 1.25 in *amip-m4K*. As the models are all
159 subject to the same SST forcing the similarities across the ensemble in the land/sea contrast
160 under both warming and cooling, and in the differences between them, are expected.

161 Using an earlier version of the Met Office Hadley Centre climate model, Joshi et al.
162 (2008) estimated a land/sea contrast of 1.4 and 1.3 under uniform 4 K warming and cooling,
163 respectively. Our results are thus consistent with their proposed mechanism to explain the
164 land/sea contrast, which applies to both global warming and cooling. The small difference
165 between the warming and cooling experiments then arises because of the inherent non-linearities
166 in this mechanism due to its dependence on the Clausius-Clapeyron relation.

167 3.2 Global-mean feedbacks

168 The global-mean net climate feedback in *amip-p4K* is less negative (i.e., less stabilizing
169 and implying a higher climate sensitivity) than under *amip-m4K* in all nine models and the
170 ensemble mean difference is 0.13 Wm^{-2} K^{-1} (Fig. 2a). For context, this difference in the feedback
171 would lead to an ensemble-mean difference of around 0.5 K in the estimated effective climate
172 sensitivity: this is discussed further in Section 6. The ensemble mean feedbacks for the two
173 experiments are summarized in Table 2.

174 The longwave clear-sky feedback is also less negative under warming in all the models
175 (Fig. 2b). Note that non-linearities in the Stefan-Boltzmann law and the Clausius-Clapeyron
176 relation mean that some asymmetry is "built in" to the experimental design. This can be
177 understood by reframing the experiments as two successive 4 K warmings, i.e., from *amip-m4K*
178 to *amip* and from *amip* to *amip-p4K*. Rather than a dependence on warming or cooling we can
179 then consider the differences as a function of the control state (cf. Colman and McAvaney,
180 2009). Starting from the warmer *amip* control state results in a more stabilising (more negative)
181 Planck feedback compared to starting from *amip-m4K*. It also leads to a stronger (more positive)
182 water vapour feedback, even though the relative humidity remains approximately constant (e.g.
183 Colman and McAvaney, 2009). In addition, if the atmosphere remains close to a moist adiabatic
184 profile with warming, the lapse rate feedback will also be stronger (more negative) when starting
185 from a warmer base state. The water vapour feedback effect thus appears to dominate the
186 longwave clear-sky feedback difference.

187 The longwave cloud feedbacks (LW CRE) lie close to the 1:1 line (Fig 2e). The robust
188 difference in the global-mean net feedback is, therefore, primarily the result of a stronger water
189 vapour feedback and a generally more positive shortwave cloud feedback (SW CRE, Fig. 2f)
190 under warming.
191
192 In two models the sign of the global shortwave cloud feedback is different under
193 warming and cooling, although the magnitude of the feedbacks is small in both cases. These are

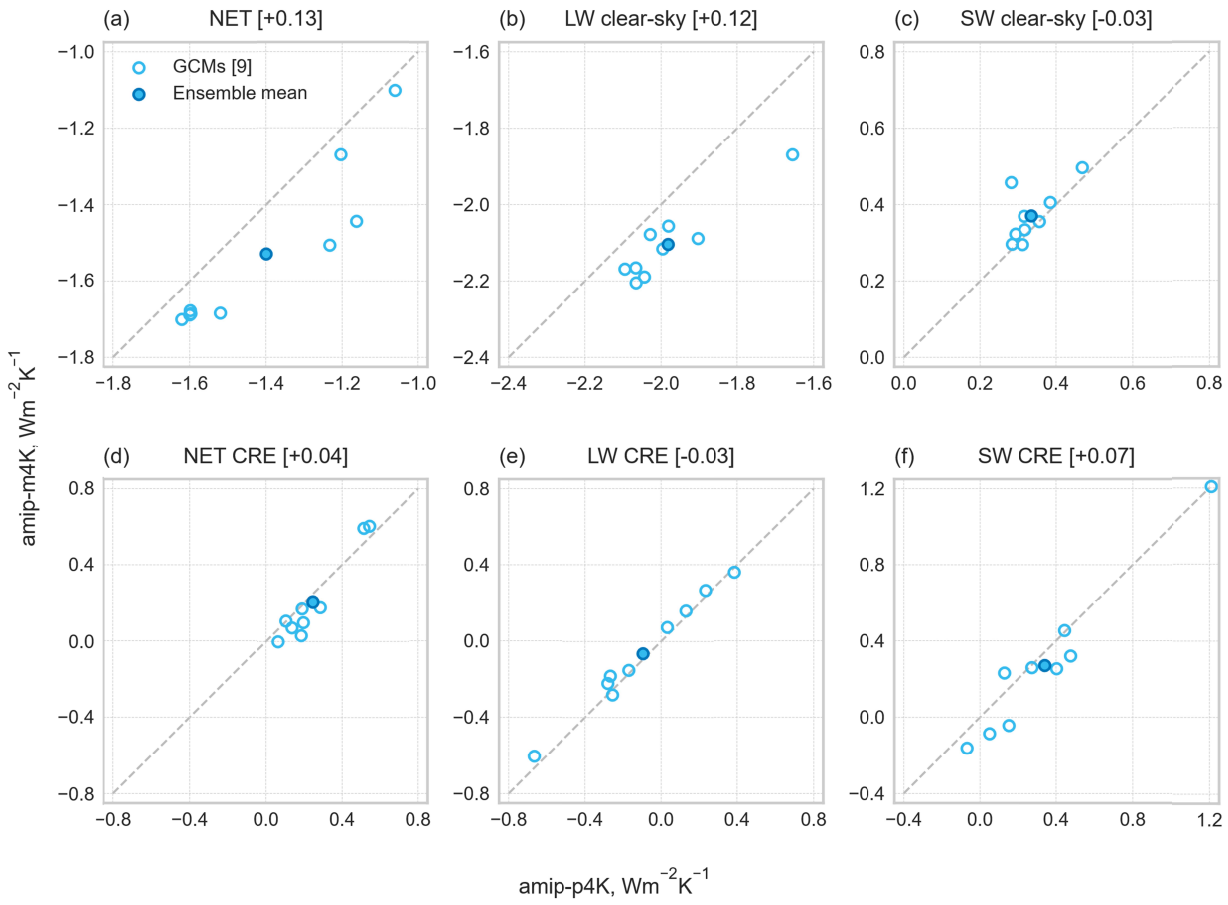

Figure 2: Global-mean feedbacks in the *amip-m4K* experiments versus the *amip-p4K* experiments. Open circles are the individual models, filled circles are the ensemble means and the ensemble mean differences (*amip-p4K* minus *amip-m4K*) are shown in the figure titles. The dashed grey line is the 1:1 line.

Table 2: Global-mean feedbacks in the *amip-p4K* and *amip-m4K* experiments. Values are the ensemble means using the nine available models. Also listed are: the p-values determined from a *t*-test to estimate the significance of the differences between *amip_p4K* and *amip_m4K*; the 2.5 and 97.5 percentiles for the differences in the ensemble-mean feedbacks (i.e. the 95% confidence range for the differences) estimated using a bootstrapping procedure.

	amip_p4K Wm^{-2} K^{-1}	**amip_m4K Wm^{-2} K^{-1}**	**p**	**P 2.5 Wm^{-2} K^{-1}**	**P 97.5 Wm^{-2} K^{-1}**
NET	-1.40	-1.53	0.0026	0.08	0.19
Longwave	-2.08	-2.17	0.0011	0.06	0.13
Shortwave	0.68	0.64	0.2927	-0.02	0.10
LW clear sky	-1.98	-2.10	0.0001	0.09	0.16
SW clear sky	0.34	0.37	0.0985	-0.07	-0.01
NET CRE	0.25	0.21	0.1472	-0.01	0.09
LW CRE	-0.10	-0.07	0.0457	-0.05	-0.01
SW CRE	0.34	0.27	0.0630	0.01	0.13

the only examples of such asymmetry at the global scale. The difference in the net cloud feedback (Fig. 2d) is thus largely determined by the shortwave component: the net cloud feedback itself is robustly positive, although it is very close to zero in one model in *amip-m4K*.

The constraint of using fixed sea ice limits the shortwave clear-sky response and the feedbacks lie close to the 1:1 line (Fig. 2c), with one exception. This is BCC-CSM2-MR model and appears to be due to an unusual response in the tropics (see below).

We have also estimated the global feedbacks from the differences between the *amip-p4K* and *amip-m4K* experiments, i.e., without reference to the control simulations (not shown). They are very close to the mean of the *amip-p4K* and *amip-m4K* feedbacks because the magnitude of the global-mean warming is similar in both cases.

The formal statistical test shows that the differences between the net, longwave, and longwave clear-sky feedbacks are significant at the 1% level (Table 2), consistent with Fig. 2. We also estimate the 95% confidence interval for the differences in the mean feedbacks using a bootstrapping procedure (resampling 10000 times with replacement). This suggests that the differences in the shortwave and longwave CRE feedbacks *may* be indicative of a robust response, i.e., the 95% confidence interval does not span zero (Table 2). However, we emphasise caution in over interpreting these findings due to the small sample size.

The "state dependence" argument described above should in principle also apply to further warming. For example, Block and Mauritsen (2013) show that the global-mean net feedback increases by 0.19 Wm^{-2} K^{-1} in their *amip-p8K* experiment compared to *amip-p4K*. Furthermore, the water vapour feedback also increases, and the combined lapse rate and Planck feedback becomes more stabilizing.

4 Regional Feedbacks

Are the differences between the global-mean feedbacks under warming and cooling representative of the regional or local responses in the models? We start by examining the zonal-mean feedbacks, focussing initially on the ensemble mean responses.

The net feedback is more positive under warming everywhere except for two relatively small sections of the tropics and sub-tropics in both hemispheres (Fig. 3a). This suggests that the global-mean difference is, to a large extent, a robust indicator of the regional behaviour. The exceptions arise from subtle differences between cancellation of the differences in the longwave clear-sky (water vapour) and cloud feedbacks (see below; Fig. 4d). In these and all subsequent plots of zonal-mean feedbacks the values are latitude weighted so that their contribution to the global mean can be more easily assessed.

The longwave clear-sky feedback difference (Fig. 3b) is largely confined to the tropics and, following the discussion above, results from the dominant effect of the difference in the water vapour feedback (more positive under warming) compared to the differences in the Planck and lapse rate feedbacks. For completeness, Figure 3c illustrates how the water vapour itself depends on the control state via the Clausius-Clapeyron relation: the relative change in the precipitable water (the vertical integral of specific humidity) is the same at all latitudes if we consider the experiments as two successive warmings starting from the cooler (*amip-m4K*) and warmer (*amip*) control states. This is also shown, though in a slightly different way, in Fig. 5(b) of Yoshimori et al. (2009).

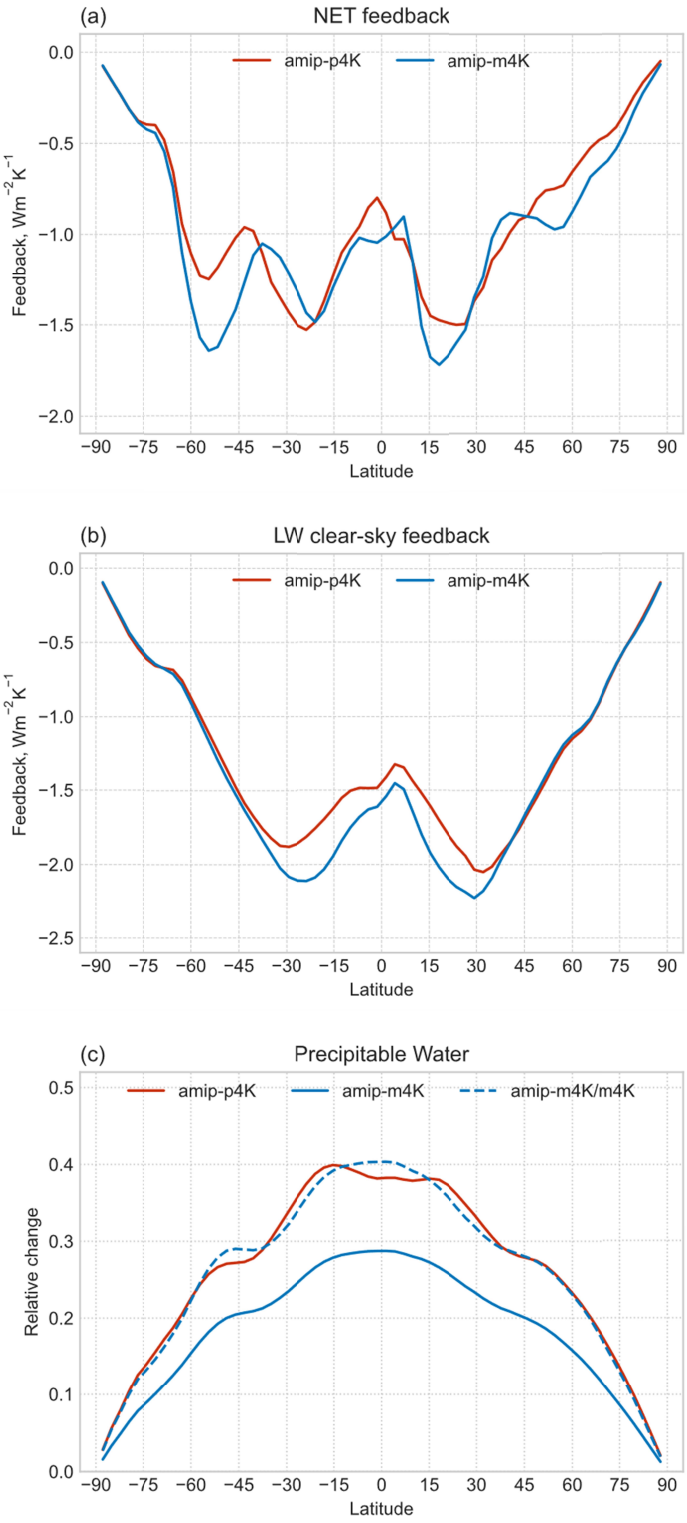

Figure 3: Ensemble mean, zonal-mean (a) net radiative feedback, (b) longwave clear-sky feedback, and (c) relative change in the precipitable water content. In (c) amip-m4K/m4K (dashed blue line) shows the relative change between *amip* and *amip-m4K* starting from *amip-m4K* as the base state.

Figs. 4a-c show how the difference in the zonal-mean net cloud feedback under warming and cooling is mainly determined by that in the shortwave component, which is again consistent with the global-mean responses. There appear to be two distinct effects: local modification of a quasi-fixed cloud distribution in the tropics (30°N – 30°S) and poleward migration with warming at higher latitudes. Examination of the zonal-mean shortwave CRE, rather than the responses, in all three experiments (not shown) indicates an approximately 3° poleward shift for each 4 K SST warming. This is based on the location of the mid-latitude minimum (largest negative) shortwave CRE in both hemispheres and is considered in more detail in Section 5. Once again, these changes can also be viewed either as responses to warming and cooling relative to the present day or as two successive warmings. For example, poleward migration with warming and equatorward migration with cooling can be thought of as further poleward migration with successive warmings. A further point of interest is that differences in the poleward shift can lead to the shortwave and net CRE feedback locally being of opposite sign in the *amip-p4K* and *amip-m4K* experiments, e.g., between around 46 – 51°S in the Southern Hemisphere.

The zonal-mean differences between the *amip-p4K* and *amip-m4K* feedbacks (Fig. 4d) illustrate two key points: (i) poleward of 40° in both hemispheres the difference in the net feedback is positive (matching the global-mean difference) and is determined primarily by the difference in the net cloud feedback; and (ii) equatorward of 40° the difference in the net feedback is determined by the degree of cancellation between the differences in the longwave clear-sky feedback (positive, due to the water vapour feedback effect) and the cloud feedback (generally negative and dominated by the shortwave component). A smaller secondary effect occurs over land in the Northern Hemisphere and results from differences in the snow retreat (not shown) in response to the warming from *amip-m4K* to *amip-p4K*.

The zonal-mean net cloud feedback in the nine individual models (Fig. 5) highlights the robustness of the ensemble mean response. Although they are not identical, the models are clearly very similar to each other and to Fig. 4c. This is also highlighted in Fig. 6, which shows how the dominance of the cloud feedback differences in the extra-tropics and the degree of cancellation between the longwave clear-sky and net CRE feedbacks in the tropics are also robust features across the ensemble.

Figure 6 also illustrates some model specific features. An unusual shortwave clear-sky feedback in the BCC-CSM2-MR model (not shown) means that the longwave clear-sky/net CRE cancellation does not apply in the tropics as it does in other models. This may be due to a similarly unusual aerosol response to cooling, but we have been unable to isolate the precise cause. IPSL-CM6A-LR has close to zero difference in the tropical net CRE feedback (Fig. 6g) due to cancellation of the shortwave and longwave effects (Fig. 5g). This results in the net feedback in the tropics being almost exactly equal to the longwave clear-sky feedback. The same behaviour, although limited to the deep tropics, also occurs in GFDL-CM4 (Figs. 6e, 5e).

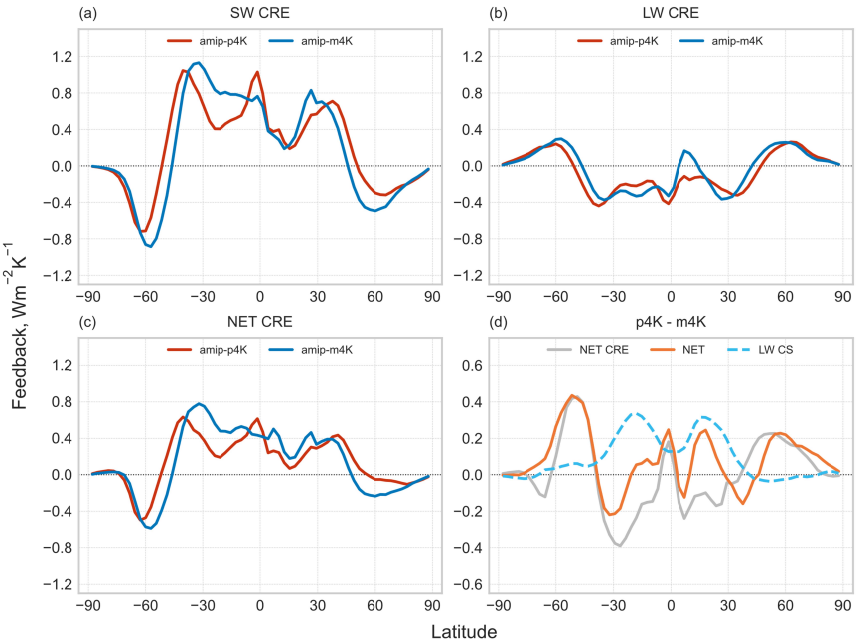

Figure 4: Ensemble mean, zonal-mean (a) shortwave, (b) longwave and (c) net CRE feedbacks in the *amip-p4K* and *amip-m4K* experiments. Differences between the *amip-p4K* and *amip-m4K* net, net CRE and longwave clear-sky feedbacks are shown in (d).

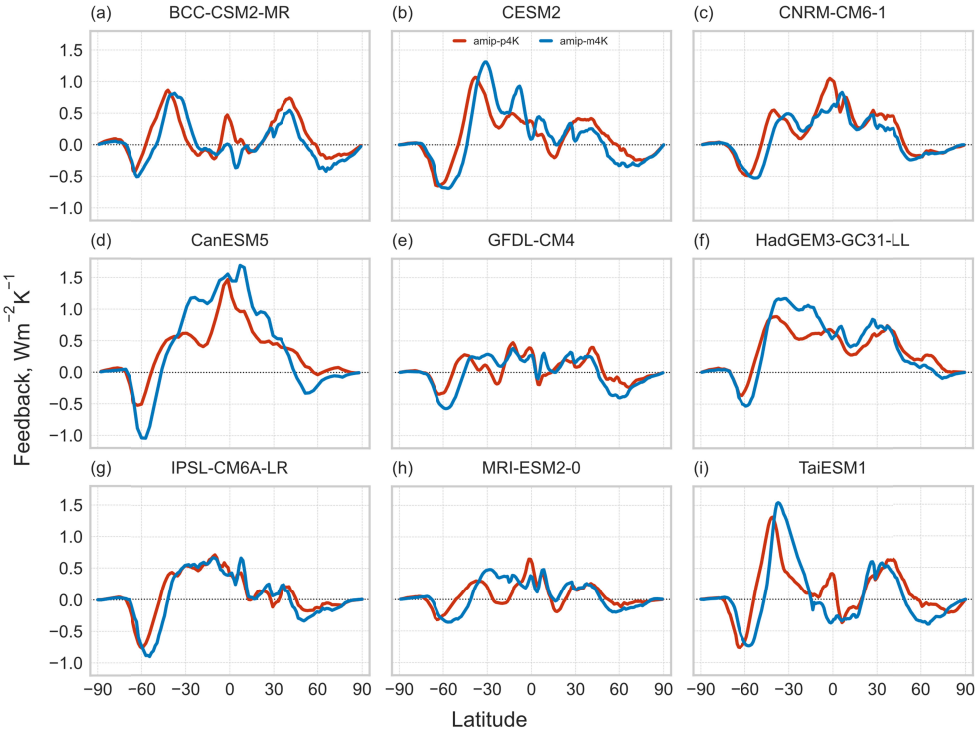

Figure 5: Annual, zonal-mean net CRE feedbacks in the *amip-p4K* and *amip-m4K* experiments for the nine individual models.

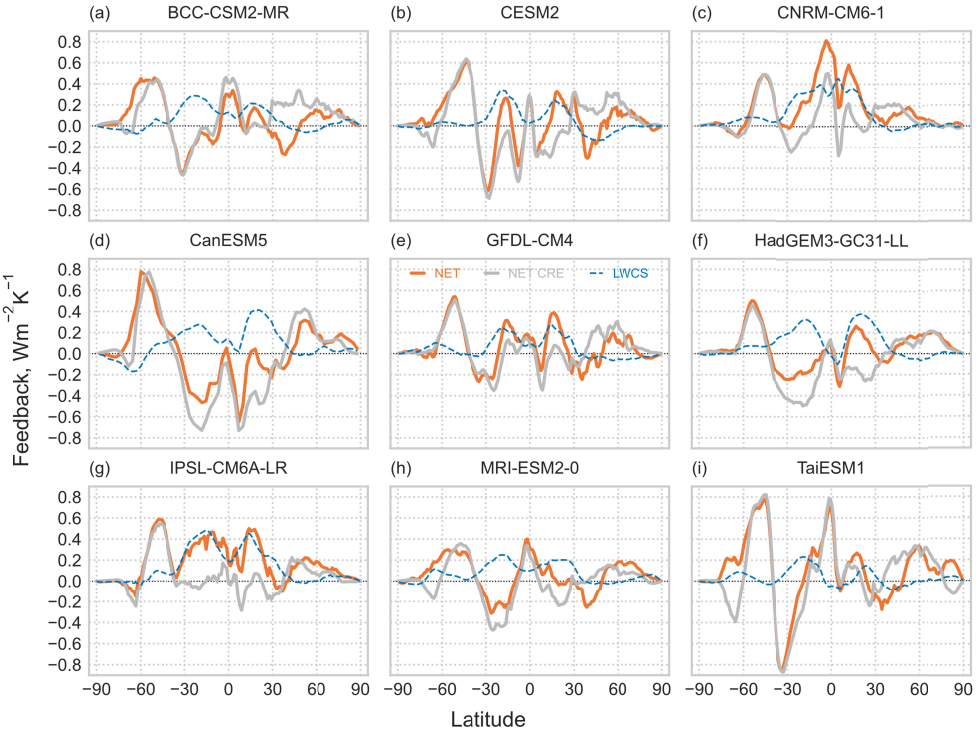

Figure 6: Differences between the net, net CRE and longwave clear-sky feedbacks in the *amip-p4K* and *amip-m4K* experiments for the nine individual models.

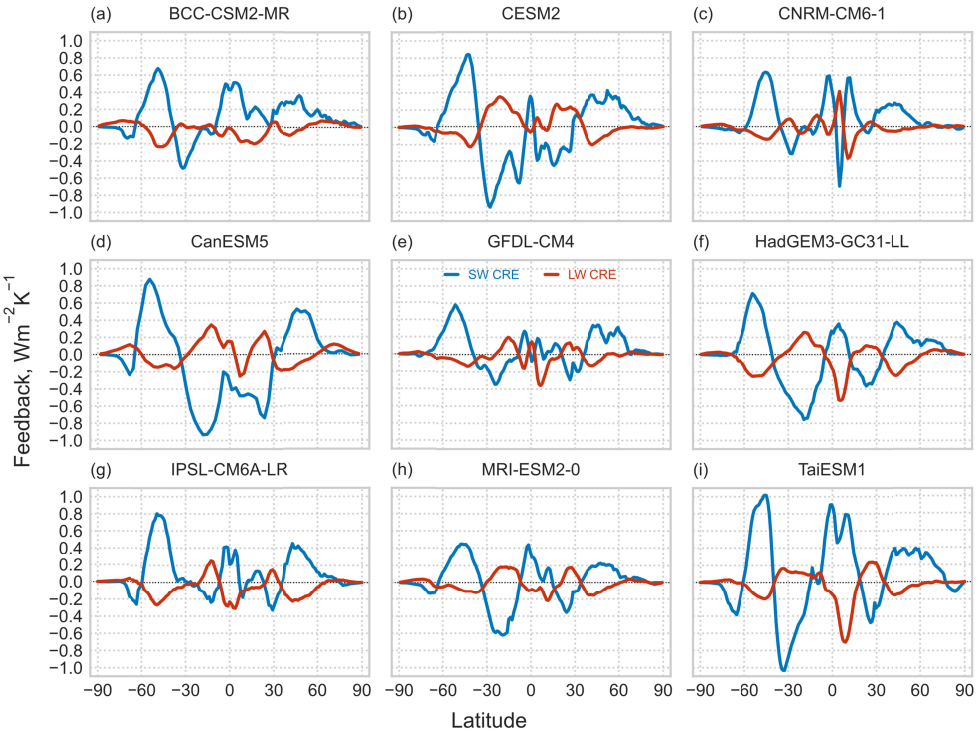

Figure 7: Differences between the shortwave and longwave CRE feedbacks in the *amip-p4K* and *amip-m4K* experiments for the nine individual models.

Yet another robust feature is shown in Fig. 7: the differences between the shortwave and longwave CRE feedbacks under warming and cooling are of opposite sign at all latitudes and in all nine models. This also means that they change sign (i.e. cross the zero line) at the same latitudes; the one notable exception is CESM2 at around 30°N. As with the ensemble mean, the difference in the net CRE feedback is largely determined by the shortwave component. Overall, we can therefore identify a clear pathway from the regional to the global behaviour regarding the differences in the cloud feedbacks under warming and cooling, which is consistent across the ensemble.

We next consider the geographical distributions of the *amip-p4K* minus *amip-m4K* feedback differences (Fig. 8). These show a high degree of zonal symmetry, particularly, for example, in the net cloud feedback difference (Fig 8c). There is greater spatial variability in the tropics, especially in the shortwave cloud feedback (Fig 8d) but also in the clear-sky longwave feedback (Fig. 8b). The largest (positive) differences in the local longwave clear-sky feedback, which, as before, are driven by the asymmetry in the water vapour feedback, are located where the climatological control longwave clear-sky flux is highest (> 290 Wm^{-2}), i.e., the driest regions. As with the zonal means, the pattern of net feedback difference (Fig. 8a) largely results from the degree of compensation between the longwave clear-sky and shortwave cloud feedbacks.

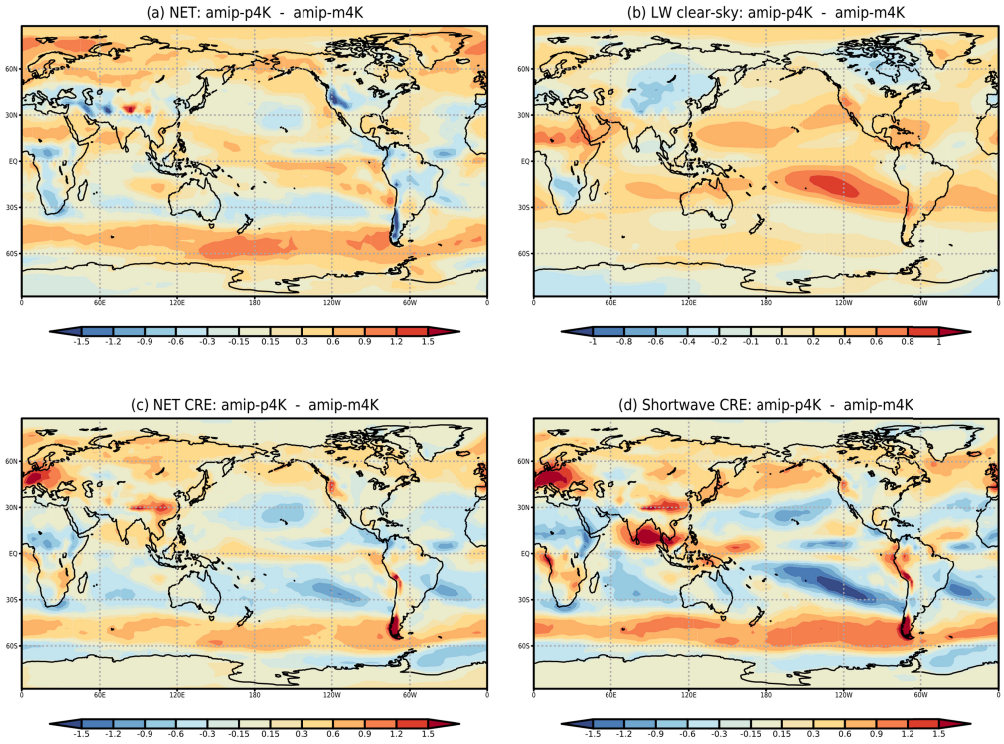

Figure 8: Differences between the ensemble-mean annual-mean (a) net, (b) longwave clear-sky, (c) net CRE and (d) shortwave CRE feedbacks in the *amip-p4K* and *amip-m4K* experiments. All in Wm^{-2} K^{-1}.

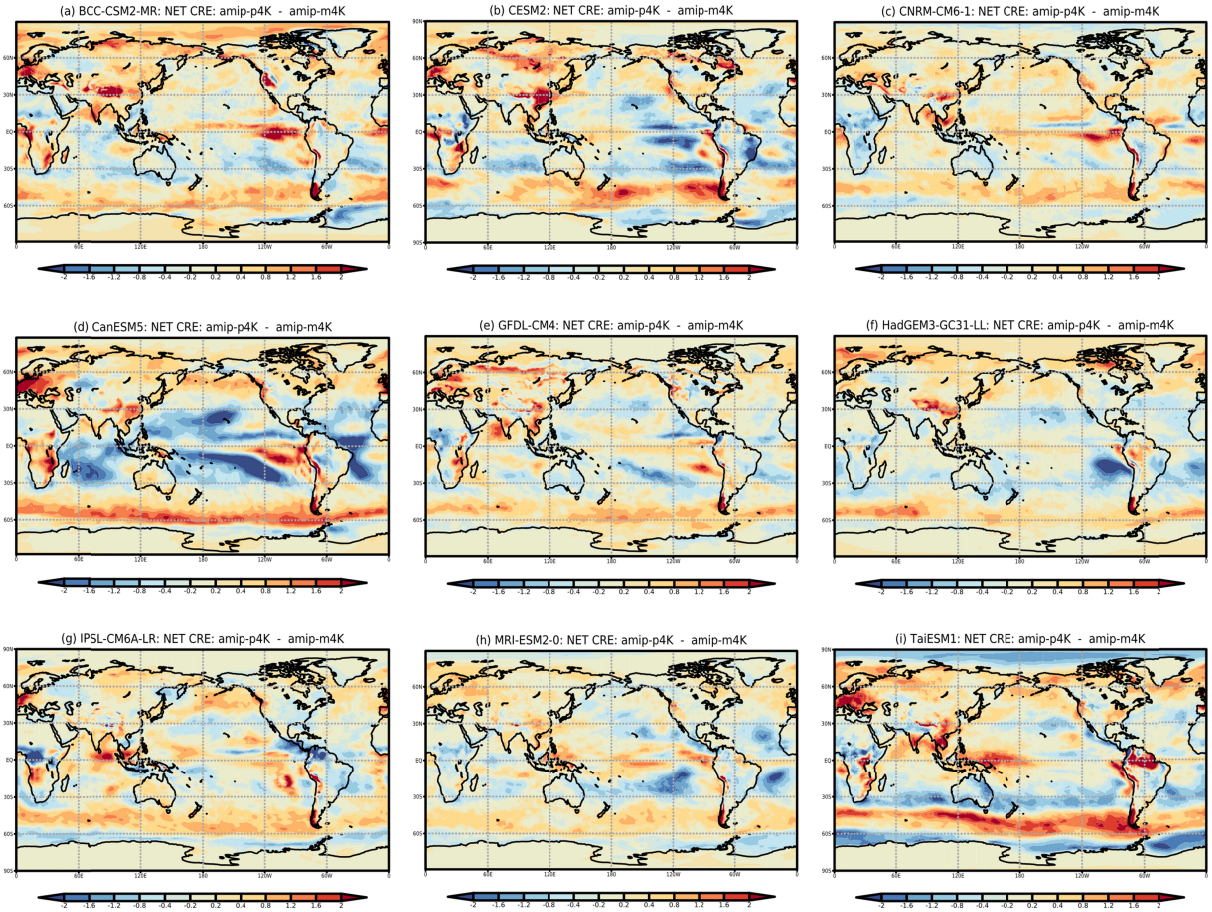

Figure 9: Differences between the net CRE feedbacks in the *amip-p4K* and *amip-m4K* experiments for the nine individual models. All in Wm^{-2} K^{-1}.

Even in this relatively small ensemble, there is considerable spatial variation in the tropical cloud feedback differences (Fig. 9), which is driven mainly by the shortwave component (not shown). Intermodel variation in the magnitude of the zonally symmetric difference in the response over the Southern Ocean (the poleward migration mentioned above) is also apparent. We again caution that large effects in one or two individual models (e.g., CanESM5 in the tropics and TaiESM1 in the Southern Hemisphere) may contribute disproportionately to the ensemble spread.

Fig. 10 confirms that the across-ensemble spread in the global-mean warming minus cooling differences is largely driven by the differences in the tropics. The picture (apparent from both zonal-mean and spatial patterns) is thus of large but robust differences in the extra-tropics, with the ensemble spread arising mainly from the diversity of the responses in the tropics. Put another way: poleward migration and the associated cloud response are robust, while tropical cloud responses (in particular, low clouds driving the shortwave cloud feedback) are subject to greater intermodel spread.

348 The relationship between the poleward migration at mid-latitudes and the responses of
349 cloud properties to the SST forcing (warming and cooling) are more clearly illustrated in Fig. 11.
350 The latter are dominated by the responses of water cloud, although the responses of ice cloud are
351 not negligible and clearly contribute to the overall response of the cloud albedo. These match up
352 with the shortwave and net cloud feedbacks, both the *amip-p4K*/*amip-m4K* feedbacks (Figs. 4a,
353 c) and their differences (Fig. 4d) in these regions. In contrast there is very little difference in the
354 cloud condensate and cloud albedo responses to warming and cooling in the tropics, which are
355 themselves far smaller than those at mid-latitudes. This suggests that both the feedbacks and the
356 differences between warming and cooling are primarily driven by changes in cloud amount
357 rather than other cloud properties.

358

359

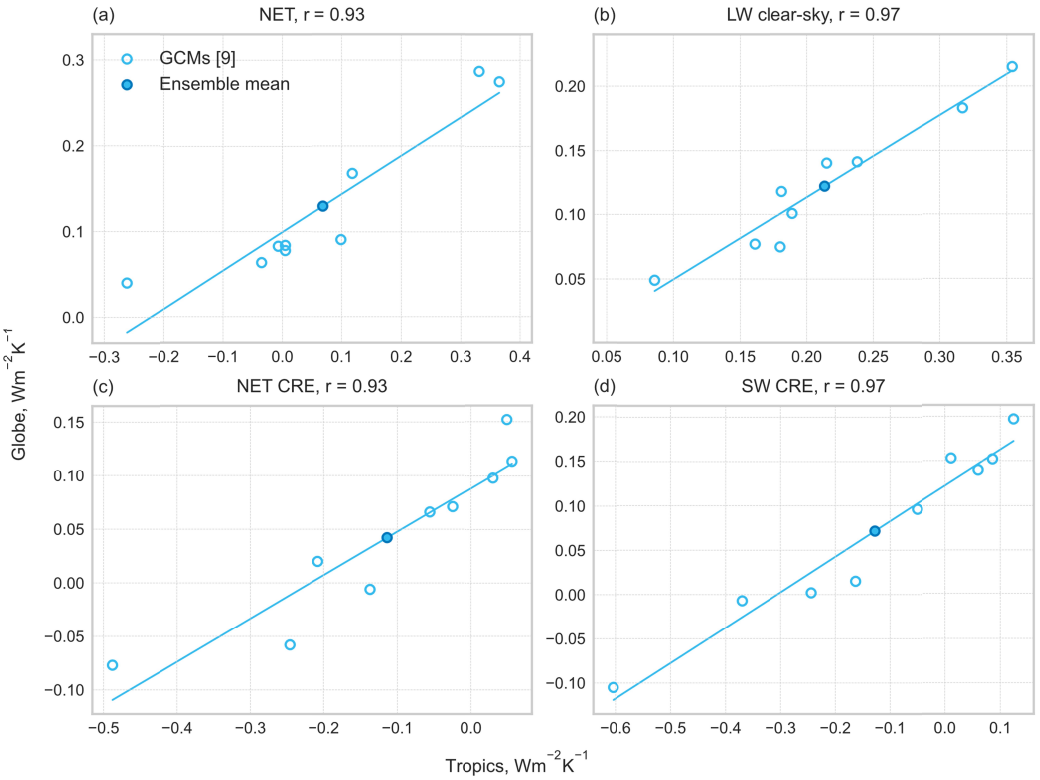

360

361 **Figure 10:** Scatterplot of the differences in the feedbacks between *amip-p4K* and *amip-m4K*, global
362 means versus tropical means. Open circles show the individual models, filled circles show the ensemble
363 means. The linear correlation coefficients are shown in the titles.

364

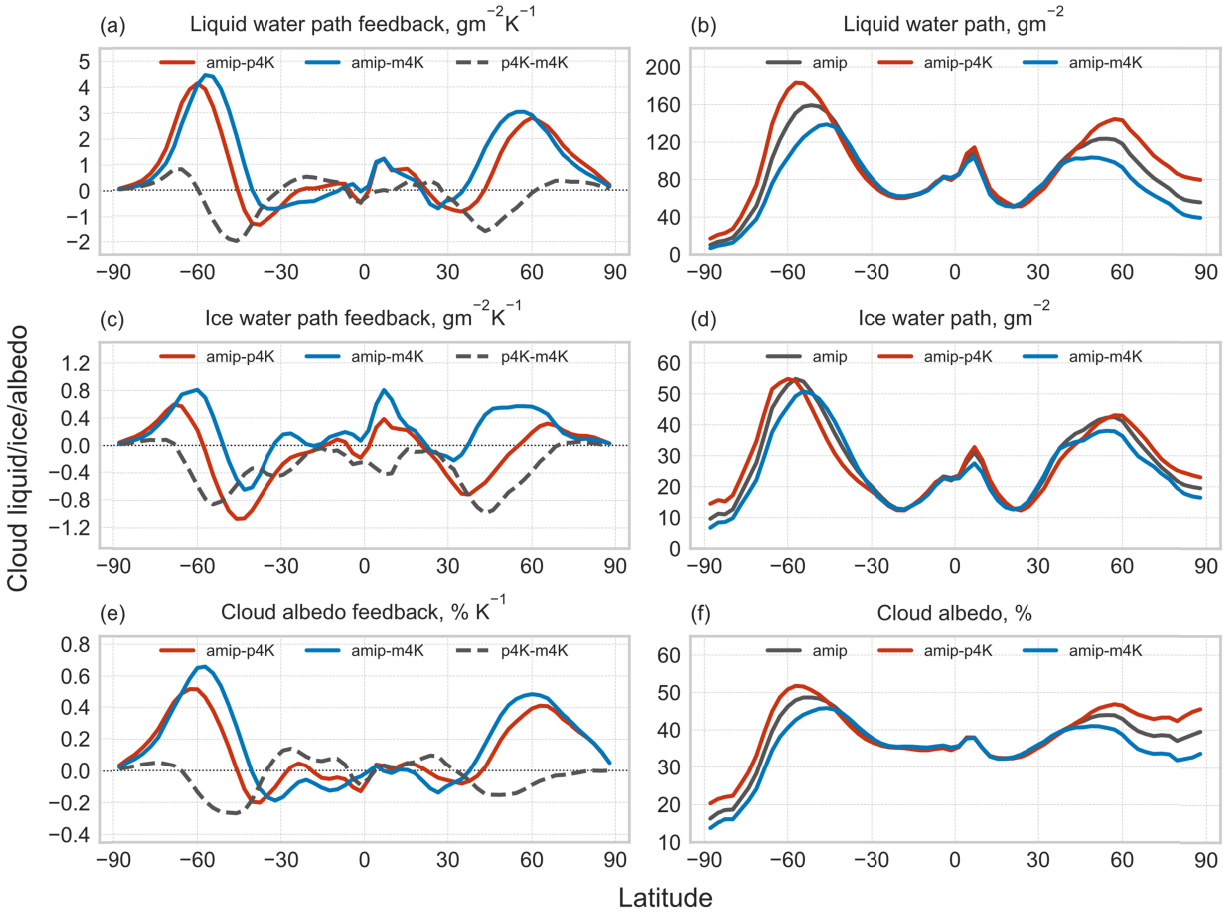

Figure 11: [Left] Ensemble-mean, zonal-mean *amip-p4K* and *amip-m4K* feedbacks in (a) cloud liquid water path, (c) cloud ice water path and (e) cloud albedo. The grey dashed line shows the difference between the *amip-p4K* and *amip-m4K* feedbacks. [Right] The ensemble mean, zonal-mean (b) cloud liquid water path, (d) ice water path and(f) cloud albedo in the *amip*, *amip-p4K* and *amip-m4K* experiments.

5 Poleward migration of the Southern Hemisphere jet

The poleward shift of the extra-tropical Southern Hemisphere jet in response to warming and the associated cloud feedback processes have received much attention (e.g., Tsushima et al., 2006; Ceppi et al., 2016; Bodas-Salcedo, 2018). Moreover, Zelinka et al. (2020) have emphasised the role of extra-tropical clouds in determining the climate sensitivity of CMIP6 models. Here we consider the asymmetric response of the shift to warming and cooling and its potential relationship to asymmetries in the cloud feedbacks over the Southern Hemisphere.

Table 3: Shift in the Southern Hemisphere jet. Negative values indicate a poleward shift. *abrupt-4xCO2* values are from Curtis et al. (2020). Shift/ΔT is the poleward shift per degree of global temperature change. The ensemble mean value of ΔT for the *abrupt-4xCO2* calculation is 6.60 K

	shift, degrees			**shift/ΔT, degrees K^{-1}**		
	amip-p4K	**amip-m4K**	**abrupt-4xCO2**	**amip-p4K**	**amip-m4K**	**abrupt-4xCO2**
BCC-CSM2-MR	-2.5	2.5	-2.7	-0.55	-0.57	-0.55
CESM2	-1.5	1.7	-2.6	-0.35	-0.41	-0.35
CNRM-CM6-1	-1.7	0.9	-2.1	-0.38	-0.20	-0.31
CanESM5	-1.7	3.0	-3.1	-0.37	-0.69	-0.39
GFDL-CM4	-2.1	2.6	-2.9	-0.46	-0.59	-0.50
HadGEM3-GC31-LL	-1.8	3.7	-2.7	-0.41	-0.87	-0.34
IPSL-CM6A-LR	-1.9	2.5	-3.9	-0.44	-0.59	-0.54
MRI-ESM2-0	-1.6	1.7	-2.1	-0.36	-0.39	-0.43
TaiESM1	-1.9	1.4		-0.41	-0.31	
Mean	**-1.86**	**2.22**	**-2.76**	**-0.41**	**-0.51**	**-0.43**
Standard deviation	**0.30**	**0.87**	**0.58**	**0.06**	**0.21**	**0.09**

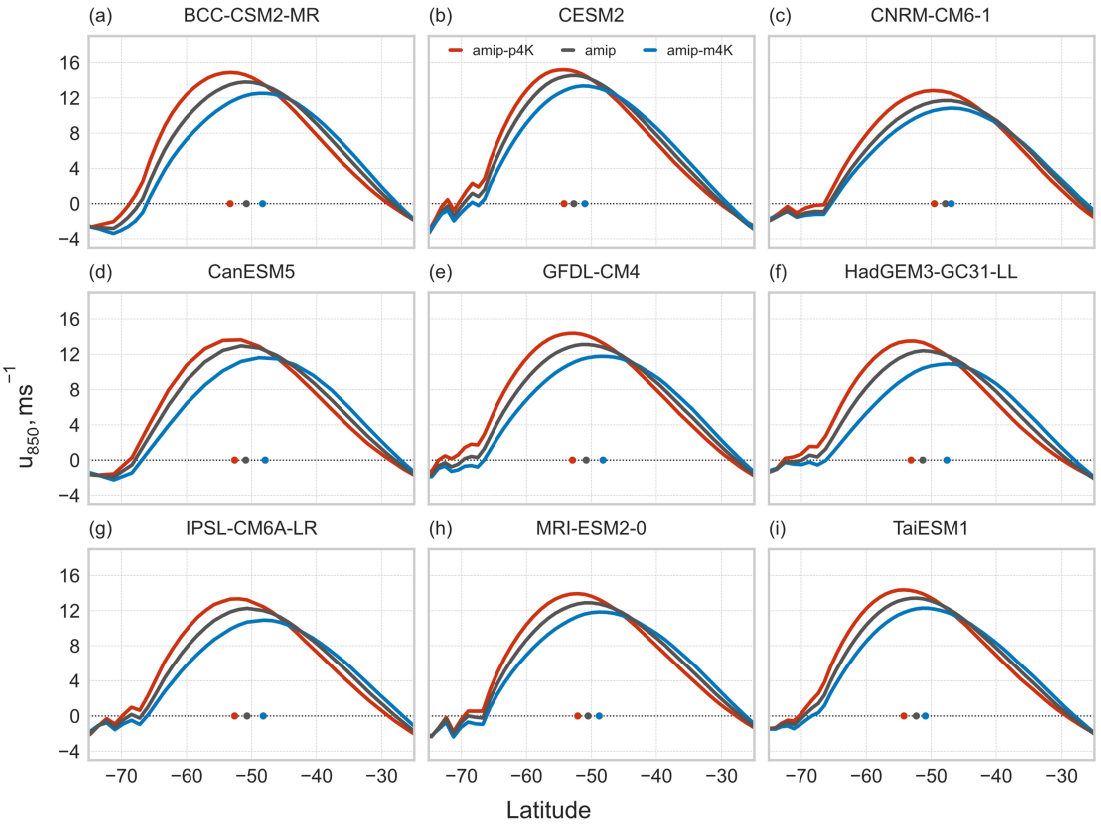

Figure 12: The zonal-mean 850 hPa zonal wind in the Southern Hemisphere in the *amip* (grey), *amip-p4K* (red) and *amip-m4K* (blue) experiments in the nine individual models. The filled circles on the zero line show the latitude of the Southern Hemisphere jet, as described in the main text.

We use the method described by Grise and Polvani (2016, 2017) to define the location of the mid-latitude eddy-driven jet as the latitude where the zonal-mean, zonal wind at 850 hPa reaches its peak value. The results are summarized in Table 3. For eight of our nine models we also include values for the *abrupt-4xCO2* experiment from Curtis et al. (2020). The shift per degree of global-mean temperature change in the coupled models under *abrupt-4xCO2* is well predicted by the *amip-p4K* experiment. This gives us confidence that the warming versus cooling comparison is legitimate.

The ensemble-mean difference in the shift between warming and cooling (0.36°) is not statistically significant (p=0.23). Some models do, however, suggest a large degree of asymmetry (Fig. 12). Models where there is a larger shift under cooling per degree of global temperature change (CanESM5, GFDL-CM4, HadGEM3-GC31-LL, IPSL-CM6A-LR) are also those which suggest the largest degree of asymmetry in the magnitude of the cloud feedback at these latitudes (cf. Fig. 5). In the remaining five models, where the asymmetry in the jet shift is small or even in the opposite sense, there is a clearly a shift in the location of the cloud feedback but the magnitude of the feedback itself remains unchanged.

To test the idea that asymmetry in the cloud feedback is related to asymmetry in the jet shift we perform uniform 4 K SST warming and cooling experiments with the aquaplanet version of the HadGEM3-GC31-LL model: we run an additional *aqua-m4K* simulation to complement the *aqua* and *aqua-p4K* simulations specified in the CFMIP protocol (Webb et al., 2017).

In the aquaplanet simulations there is a symmetric shift in the jet location under warming and cooling, regardless of the metric chosen to identify the jet position (Table 4, Fig. 13). In contrast the shift in the *amip-p4K*/*amip-m4K* simulations is asymmetric using all metrics, even when controlling for the possible influence of the time of year and a different solar insolation (the aquaplanet simulations are for perpetual September).

However, there is still an asymmetric response in the magnitude of the cloud feedbacks under warming and cooling in the aquaplanet (Fig. 14) and the aquaplanet also reproduces the anticorrelation between the shortwave and longwave CRE feedbacks at all latitudes (cf. Figs 6 and 7). This suggests that the asymmetry in the cloud feedback – when considering the annual-mean, zonal-mean response – is not driven by the jet shift and is more likely to be a thermodynamic, rather than a dynamic, response (Ceppi et al., 2014; Ceppi and Hartmann, 2015).

The hypothesis that the asymmetry in the jet location is driving that in the cloud feedbacks is thus not supported by our aquaplanet warming and cooling experiments, although this clearly needs to be tested in other models. The asymmetry in the jet shift between the *amip-p4K* and *amip-m4K* simulations presumably arises because of the presence of Antarctica and the global circulation's response to the fact that the land warms more in *amip-p4K* than it cools under *amip-m4K* (Fig 1; Table 1), including over Antarctica.

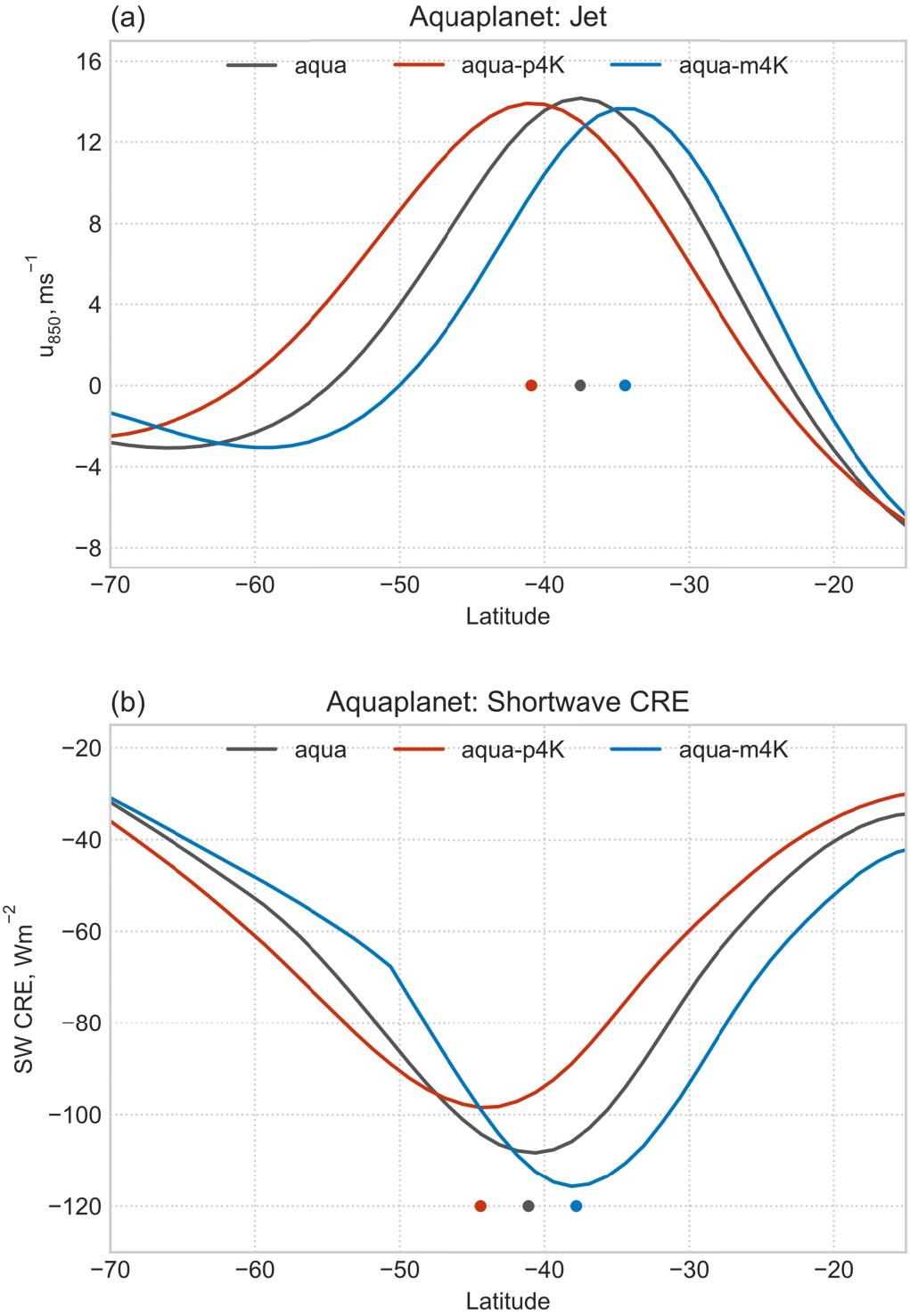

Figure 13: (a) The zonal-mean zonal wind at 850 hPa in the HadGEM3-GC31-LL *aqua*, *aqua-p4K* and *aqua-m4K* experiments, with the location of the jet shown on the zero line. (b) The zonal-mean shortwave CRE in the *aqua*, *aqua-p4K* and *aqua-m4K* experiments, with the location of the minimum shown on the y = -120 line.

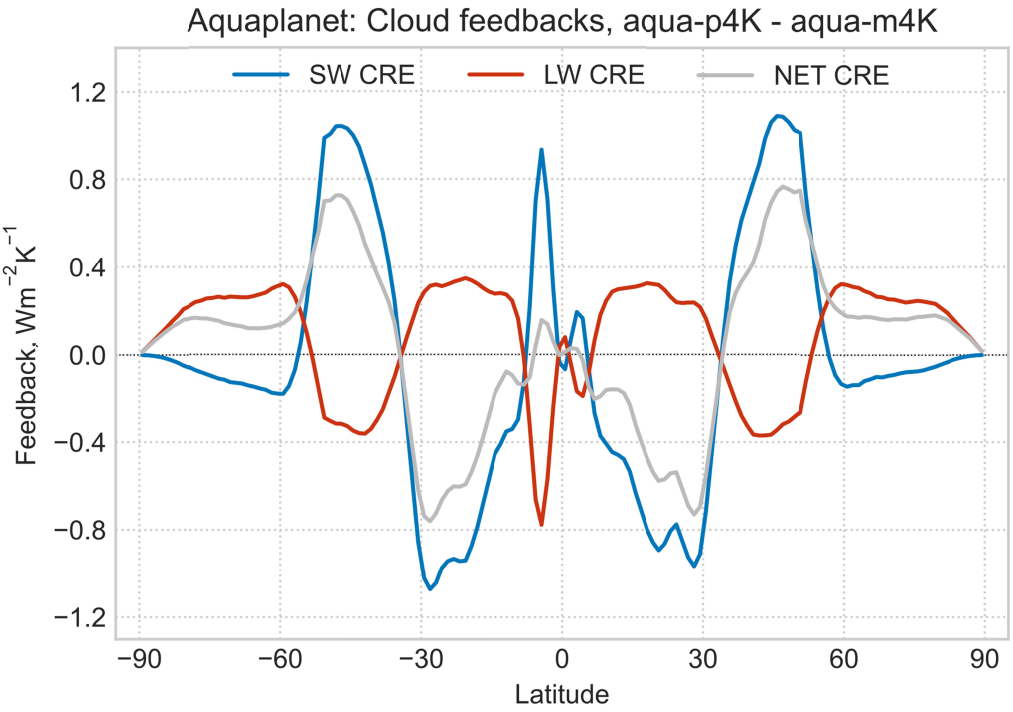

Figure 14: Differences between the shortwave, longwave and net CRE feedbacks between the HadGEM3-GC31-LL *aqua-p4K* and *aqua-m4K* experiments.

Table 4: Shift in the Southern Hemisphere jet latitude in HadGEM3-GC31-LL, indicating whether the shift is either symmetric (✓) or asymmetric (×) to warming and cooling. The location of the jet is defined using zonal wind at 850 hPa (see text) and also the shortwave cloud radiative effect (SW CRE), the cloud liquid water path (LWP) and the cloud ice water path (IWP).

	u_{850}	SW CRE	LWP	IWP
amip_p4K/m4K: annual	×	×	×	×
amip_p4K/m4K: September	×	×	×	×
aqua_p4k/m4k	✓	✓	✓	✓

6 Climate sensitivity and comparison with coupled model feedbacks

6.1 Effective climate sensitivity

We now consider the impact of the differences in the global-mean feedback between *amip-p4K* and *amip-m4K* (Section 1) on estimates of the effective climate sensitivity, S (Sherwood et al., 2020). We take the radiative forcing to be 3.47 Wm^{-2} K^{-1}: this is the ensemble mean value of the intercept of the Gregory plot using 150 years of data from the models' corresponding *abrupt-4xCO2* experiments. To account for the absence of polar amplification and the sea-ice feedback in the uniform SST experiments we replace the clear-sky shortwave feedback with the ensemble mean value from the *abrupt-4xCO2* experiments. We then obtain an ensemble mean value for S of 3.53 K in *amip-p4K* compared to 3.03 K in *amip-m4K*, i.e., the differences in the feedbacks which are represented in the uniform SST experiments lead to a 0.5 K higher sensitivity under warming ($p=0.002$). There are, though, large contributions from both the CNRM-CM6-1 and IPSL-CM6A-LR models, with differences of 0.97 and 1.16 K respectively. Excluding these, the mean difference in S reduces to 0.34 K ($p<0.001$) for the remaining seven models. In both models the large difference in the global feedback which leads to that in the estimate of S arises from a combination of the differences in the longwave clear-sky and shortwave cloud feedbacks.

The surface albedo feedback is, however, known to weaken, i.e., become less positive, for warmer climates (e.g., Colman and McAvaney, 2009). To try and account for this effect we recalculate S in the uniform SST experiments, but this time replace the shortwave clear-sky feedback in *amip-p4K* and *amip-m4K* by the ensemble mean values from the *abrupt-2xCO2* and *abrupt-0.5xCO2* experiments respectively. This results in a *lower* sensitivity estimate from the *amip_p4K* experiment (3.81 K) compared to *amip_m4K* (4.22 K).

How plausible is this? Using the same forcing of 3.47 Wm^{-2} K^{-1} together with the global feedbacks from the *abrupt-2xCO2* and *abrupt-0.5xCO2* experiments gives estimates for S of 3.54 and 4.04 K respectively, compared to the actual values of 3.69 and 3.41 K respectively. The impact of the stronger positive shortwave clear-sky feedback in *abrupt-0.5xCO2* is compensated by the opposing effects of the longwave clear-sky and shortwave cloud feedbacks (Fig. 15 below). The larger forcing in the *abrupt-2xCO2* experiment (3.65 versus 3.04 Wm^{-2} K^{-1}) then dominates the difference in the sensitivities. The difference in the forcing is comparable to that in the greenhouse gas forcing between 2xCO2 and the LGM (e.g., Sherwood et al., 2020; Zhu and Poulsen, 2021) and the impact – roughly equal net feedbacks but increased sensitivity – is consistent with that reported by Yoshimori et al. (2009). More recently, Mitevski et al. (2022) described *abrupt-2xCO2/0.5xCO2* experiments with the CESM-LE and GISS-E2.1-G models. They found little difference between the net feedbacks under 2xCO2 and 0.5xCO2 due to compensation between the various components. There was, however, still significantly increased warming under 2xCO2 due to the larger forcing. Using the CESM1 model, Chalmers et al. (2022) also found greater warming under 2xCO2 compared to 0.5xCO2 but they ascribed this to approximately equal contributions from increased forcing and a less stabilizing net feedback. They similarly noted a compensation between the differences in the feedbacks: more stabilizing non-cloud feedbacks offset by a more positive shortwave cloud feedback, with the longwave cloud feedback remaining roughly unchanged.

These estimates are, of course, only illustrative of the potential impact on S of the differences in the feedbacks alone under warming and cooling. They are not definitive estimates

of the effective climate sensitivity but show how the uniform SST experiments, if used carefully, can capture aspects of the behaviour seen in the fully coupled system. Qin et al. (2022) discuss the separate issue of which of the various combinations of forcings and feedbacks from the idealised experiments give the best estimate of models' actual climate sensitivities.

6.2 Feedbacks in coupled models

Estimates of ECS from the uniform warming/cooling experiments are clearly problematic because of the need to compensate for the lack of sea-ice feedbacks and to make assumptions about the forcing. Some feedbacks can, however, be more consistently compared with those in the fully coupled system. This is especially true for cloud feedbacks, as demonstrated by both Ringer et al. (2014) and Qin et al. (2022). Note that the emphasis here is on whether the uniform SST experiments can capture the differences between feedbacks under warming and cooling obtained using the coupled models.

Here we compare *amip-p4K* minus *amip-m4K* feedback differences with those derived from scenarios of increasing/reducing atmospheric CO_2 and increasing/reducing the solar constant (Fig. 15). The clearest feature is that the longwave CRE feedback is almost invariant to warming and cooling and this appears to be independent of the nature of the forcing (Fig. 15a). The behaviour of the shortwave (Fig. 15b) and the net CRE (Fig. 15c) feedbacks is more complex: this limited set of models suggests that the SW CRE feedback departs further from the 1:1 line than suggested by the *amip-p4K/m4K* comparison, for example. The general tendency is for both the SW and net CRE feedbacks to be more amplifying (more positive or less negative) under warming (cf. Yoshimori et al., 2009). The longwave clear-sky feedback is consistently more positive, i.e., less stabilizing, in response to warming (Fig. 15d), consistent with the dominant impact on the water vapour feedback (Colman and McAvaney, 2009) which is captured by the uniform SST experiments.

A thorough understanding of these relationships obviously requires further, more detailed, investigation. For example, the behaviour of the longwave CRE feedback may be related to the robust nature of the fixed anvil temperature (FAT) hypothesis relating to high clouds (Zelinka and Hartmann, 2010); and the diversity of the shortwave and net CRE feedback differences (exemplified by Fig. 9) could be a further manifestation of longstanding uncertainties in tropical and subtropical low cloud feedbacks (Boucher et al., 2013). Nonetheless, these initial comparisons suggest that useful insights into the coupled model feedbacks under warming and cooling scenarios could be determined from the uniform SST experiments.

There are, of course, added complexities when proper account is taken of the radiative forcing and its potential effects on the feedbacks (Zhu and Poulsen, 2021). These should not be underestimated, but the simplified experiments help to isolate both the nature of differences in feedbacks between warming and cooling and to understand the physical mechanisms associated with them. A particular advantage is that they allow a cleaner diagnosis of the regional feedbacks than is possible in the coupled experiments. For example, there is no need for regional regressions and their associated, often large, uncertainties

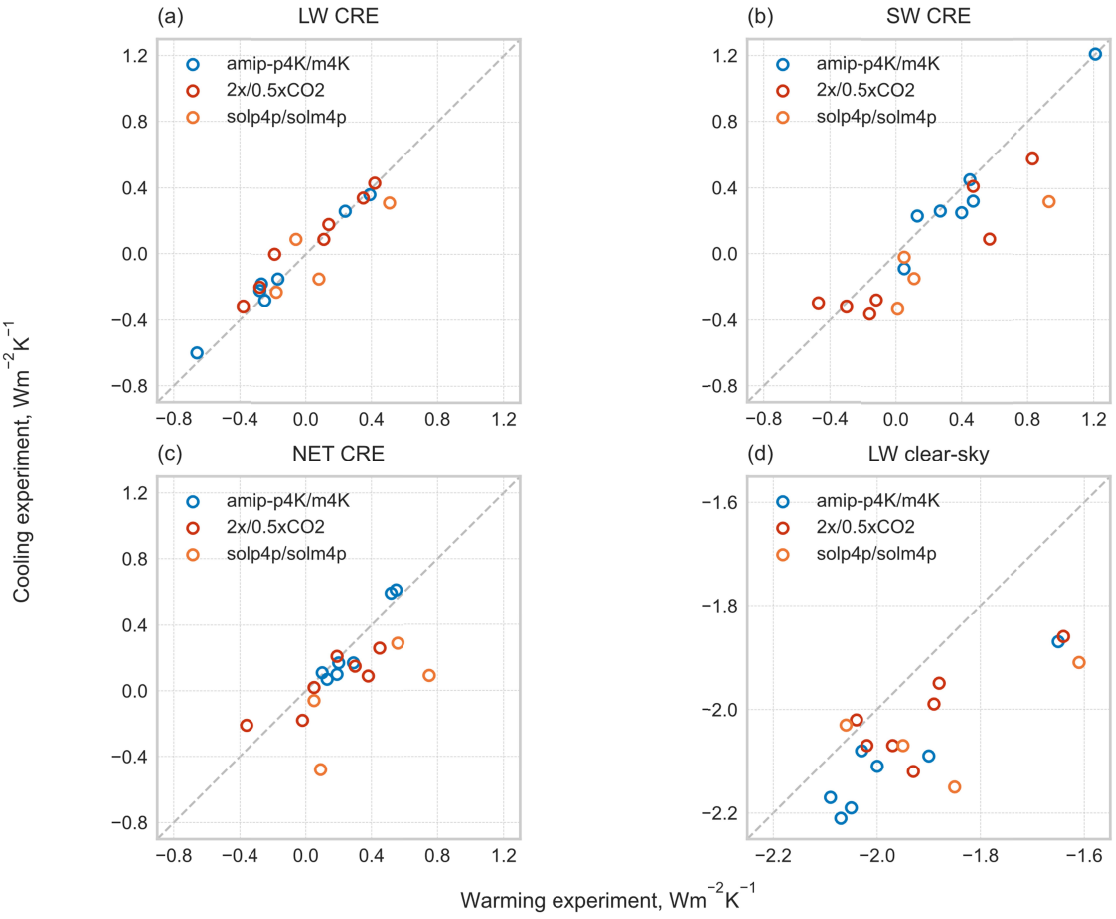

Figure 15: Comparison of the (a) LW CRE, (b) SW CRE, (c) net CRE and (d) LW clear-sky feedbacks in the *amip-p4K*/*amip-m4K, abrupt-2xCO2*/*abrupt-0.5xCO2* and *abrupt-solp4p*/*abrupt-solm4p* experiments.

7 Conclusions

We have shown that the uniform SST+4K and SST-4K experiments help to simplify the framework for understanding the climate's response to global warming and cooling and provide insights into possible asymmetries in the resulting climate feedbacks. They thus provide a useful reference (or baseline) for understanding more realistic scenarios of warming and cooling in past and future climates. This is consistent with previous work demonstrating the utility of uniform warming experiments and extends that framework to a cooling climate.

We have focussed primarily on the *differences* between the feedbacks in response to warming and cooling and to the robust behaviour across our nine-member ensemble. In this context, asymmetries are predominantly *differences in magnitude* between feedbacks of the *same sign* under warming and cooling. Our main results are:

- The global-mean net feedback is robustly less stabilising (less negative) under warming compared to cooling, and to first order this is driven by the same behaviour in the longwave clear-sky feedback.
- The difference in the longwave clear-sky feedback results from the dominance of water vapour feedback and can be understood in terms of basic physical arguments.
- The large difference in cloud feedbacks in the extra-tropics is a consistent feature across our ensemble.
- There is far more intermodel spread in tropical cloud feedbacks, which is then the principal driver of the spread in the global-mean cloud feedbacks.
- A subset of models indicates relatively large asymmetries in the Southern Hemisphere jet shift under warming and cooling; however, aquaplanet experiments with the HadGEM3-GC31-LL model suggest that this is not driving the asymmetry in the cloud feedbacks at these latitudes.
- The *amip-p4K* and *amip-m4K* experiments provide useful insights into other coupled warming/cooling scenarios; an example is the global longwave cloud feedback, which appears to be almost invariant to warming and cooling under different types of forcing (both CO_2 and solar-forced).

We also note that:

- Aquaplanet experiments provide a useful, and even more simplified, baseline for understanding the differences between responses to warming and cooling; the *aqua_m4K* experiment could therefore be a worthwhile addition to CFMIP.
- The idealised framework used here could be extended to atmosphere-only runs forced with, e.g., LGM SSTs and 2xCO2 SSTs from coupled models to compare the impact of SST patterns on the feedback differences; this is similar to the "time slice" experiments in CFMIP (Webb et al., 2017).
- For equilibrium experiments such as these, it is often more instructive to think of them as successive warmings rather than a warming and cooling; in this case one may then also refer to the asymmetry as a "state dependence".

- Cooling experiments offer an important extra dimension with which to explore the responses of global climate models to forcing and the associated feedbacks, and for testing hypotheses related to the mechanisms driving these processes.

Acknowledgments

MAR was supported by the European Union's Horizon 2020 research and innovation programme under grant agreement No 820829 (CONSTRAIN project). MAR, AB-S and MJW were supported by the Met Office Hadley Centre Climate Programme funded by BEIS. MAR thanks William Ingram for useful discussions on the interpretation of the global-mean feedbacks. We acknowledge the World Climate Research Programme, which, through its Working Group on Coupled Modelling, coordinated and promoted CMIP6. We thank the climate modelling groups for producing and making available their model output, the Earth System Grid Federation (ESGF) for archiving the data and providing access, and the multiple funding agencies who support CMIP6 and ESGF.

Data Availability Statement

All of the CMIP data used in this study are archived at https://esgf-node.llnl.gov/projects/cmip6/. The HadGEM3-GC31-LL aqua_m4K simulation data can be made available on request.

References

Bloch-Johnson, J., Rugenstein, M., Stolpe, M. B., Rohrschneider, T., Zheng, Y., & Gregory, J. M. (2021). Climate sensitivity increases under higher CO_2 levels due to feedback temperature dependence. *Geophys. Res. Lett.*, 48(4), e2020GL089074, https://doi.org/10.1029/2020GL089074

Block, K., and Mauritsen, T. (2013), Forcing and feedback in the MPI-ESM-LR coupled model under abruptly quadrupled CO_2, *J. Adv. Model. Earth Syst.*, 5, 676–691, doi:10.1002/jame.20041.

Bodas-Salcedo, A. (2018). Cloud condensate and radiative feedbacks at midlatitudes in an aquaplanet. *Geophys. Res. Lett.*, 45, 3635–3643, https://doi.org/10.1002/2018GL077217

Boucher, O., Randall, D. et al. (2013). Clouds and aerosols. In *Climate Change 2013: The Physical Science Basis. Contribution of Working Group I to the Fifth Assessment Report of the Intergovernmental Panel on Climate Change*. T.F. Stocker et al., Eds., *Cambridge University Press*, pp. 571-657, doi:10.1017/CBO9781107415324.016.

Cess, R. D., et al. (1990). Intercomparison and interpretation of climate feedback processes in 19 atmospheric general circulation models, *J. Geophys. Res.*, 95(D10), 16601–16615, doi:10.1029/JD095iD10p16601

Ceppi, P., Zelinka, M. D., and Hartmann, D. L. (2014). The response of the Southern Hemispheric eddy-driven jet to future changes in shortwave radiation in CMIP5, *Geophys. Res. Lett.*, 41, 3244–3250, doi:10.1002/2014GL060043.

Ceppi, P., Hartmann, D. L. (2015). Connections Between Clouds, Radiation, and Midlatitude Dynamics: a Review. *Curr Clim Change Rep,* 1, 94–102, https://doi.org/10.1007/s40641-015-0010-x

Ceppi P., Hartmann D. L., Webb M. J. (2016). Mechanisms of the negative shortwave cloud feedback in middle to high latitudes, *Journal of Climate*, 29, 139-157, https://doi.org/10.1175/JCLI-D-15-0327.1

Chalmers, J., Kay, J. E., Middlemas, E., Maroon, E. and DiNezio, P. (2022). Does disabling cloud radiative feedbacks change spatial patterns of surface greenhouse warming and cooling? *Journal of Climate*, 35, 1787 –1807, https://doi.org/10.1175/JCLI-D-21-0391.1

Colman, R., and McAvaney, B. (2009). Climate feedbacks under a very broad range of forcing, *Geophys. Res. Lett.*, 36, L01702, doi:10.1029/2008GL036268.

Curtis P. E., Ceppi P., Zappa G. (2020). Role of the mean state for the Southern Hemispheric Jet Stream response to CO_2 forcing in CMIP6 models, *Environmental Research Letters*, 15, 1-7, https://10.1088/1748-9326/ab8331

Gregory, J. M., Ingram, W. J., Palmer, M. A., Jones, G. S., Stott, P. A., Thorpe, R. B., & Williams, K. D. (2004). A new method for diagnosing radiative forcing and climate sensitivity. *Geophys. Res. Lett.*, 31(3), https://doi.org/10.1029/2003GL018747

Grise, K. M. and Polvani, L. M. (2016). Is climate sensitivity related to dynamical sensitivity?, *J. Geophys. Res. Atmos.*, 121, 5159– 5176, doi:10.1002/2015JD024687.

Grise, K. M. and Polvani, L. M. (2017). Understanding the time scales of the tropospheric circulation response to abrupt CO2 Forcing in the Southern Hemisphere: Seasonality and the Role of the Stratosphere, *Journal of Climate*, 30(21), 8497-8515, https://doi.org/10.1175/JCLI-D-16-0849.1

Joshi, M. M., Gregory, J. M., Webb, M. J., Sexton, D. M. H., and Johns, T. C. (2008). Mechanisms for the land/sea warming contrast exhibited by simulations of climate change, *Clim. Dyn.*, 30, 455–465.

Mitevski, I., Polvani, L. M., & Orbe, C. (2022). Asymmetric warming/cooling response to CO_2 increase/decrease mainly due to non-logarithmic forcing, not feedbacks. *Geophys. Res. Lett.*, 49, e2021GL097133, https://doi.org/10.1029/2021GL097133

Qin, Y., Zelinka, M. D., & Klein, S. A. (2022). On the correspondence between atmosphere-only and coupled simulations for radiative feedbacks and forcing from CO_2. *J. Geophys. Res. Atmos.*, 127, e2021JD035460, https://doi.org/10.1029/2021JD035460

Ringer, M. A., et al. (2006). Global mean cloud feedbacks in idealized climate change experiments, *Geophys. Res. Lett.*, 33, L07718, doi:10.1029/2005GL025370.

Ringer, M. A., Andrews, T., and Webb, M. J. (2014). Global-mean radiative feedbacks and forcing in atmosphere-only and coupled atmosphere-ocean climate change experiments, *Geophys. Res. Lett.*, 41, 4035–4042, doi:10.1002/2014GL060347

Schneider, S. H., Washington, W. M., and Chervin, R. (1978). Cloudiness as a climatic feedback mechanism: Effects on cloud amounts of pre- scribed global and regional surface temperature change in the NCAR GCM, *J. Atmos. Sci.*, 35, 2207-2221.

Sherwood, S. C., Webb, M. J., Annan, J. D., Armour, K. C., Forster, P. M., Hargreaves, J. C., et al. (2020). An assessment of Earth's climate sensitivity using multiple lines of evidence. *Reviews of Geophysics*, 58(4), https://doi.org/10.1029/2019RG000678

Tsushima, Y., Emori, S., Ogura, T., Kimoto, M., Webb, M. J., Williams, K. D., et al. (2006). Importance of the mixed-phase cloud distribution in the control climate for assessing the response of clouds to carbon dioxide increase: A multi-model study. *Climate Dynamics*, 27(2-3), 113–126, https://doi.org/10.1007/s00382-006-0127-7

Webb, M. J., Andrews, T., Bodas-Salcedo, A., Bony, S., Bretherton, C. S., Chadwick, R., et al. (2017). The Cloud Feedback Model Intercomparison Project (CFMIP) contribution to CMIP6. *Geoscientific Model Development*, 10(1), 359–384, https://doi.org/10.5194/gmd-10-359-2017

Yoshimori, M., Yokohata, T., and Abe-Ouchi, A. (2009). A comparison of climate feedback strength between CO_2 doubling and LGM experiments. *Journal of Climate,* 22(12), 3374-3395, https://doi.org/10.1175/2009JCLI2801.1

671 Zelinka, M. D., and Hartmann, D. L. (2010). Why is longwave cloud feedback positive? *J.*
672 *Geophys. Res.*, 115, D16117, doi:10.1029/2010JD013817.
673 Zelinka, M. D., Myers, T. A., McCoy, D. T., Po-Chedley, S., Caldwell, P. M., Ceppi, P., et al.
674 (2020). Causes of higher climate sensitivity in CMIP6 models. *Geophys. Res.*
675 *Lett.*, 47(1), https://doi.org/10.1029/2019GL085782
676 Zhu, J. and Poulsen, C. J. (2021). Last Glacial Maximum (LGM) climate forcing and ocean
677 dynamical feedback and their implications for estimating climate sensitivity, *Clim. Past,* 17,
678 253–267, https://doi.org/10.5194/cp-17-253-2021.
679